INSTITUTE OF PHYSICS PUBLISHING SUPERCONDUCTOR SCIENCE AND TECHNOLOGY

Supercond. Sci. Technol. **15** (2002) 307–314 PII: S0953-2048(02)28017-3

Nonlocal electrodynamics of Josephson junctions in thin films and fractional vortices

R G Mints and Ilya Papiashvili

School of Physics and Astronomy, Raymond and Beverly Sackler Faculty of Exact Sciences, Tel Aviv University, Tel Aviv 69978, Israel

Received 17 August 2001
Published 25 January 2002
Online at stacks.iop.org/SUST/15/307

Abstract

The phase difference φ across a Josephson junction is considered for a film with a thickness $d \ll \lambda$, where λ is the London penetration depth in the superconducting banks. Special attention is given to the case of a critical current density j_c varying along the junction. It is shown that a nonlinear integro-differential equation determines the spatial distribution of φ for $d \ll \lambda$. Josephson properties of grain boundaries in thin-YBCO films are treated for the case of j_c alternating along these boundaries. It is shown that if the typical amplitude of alternations of j_c is high compared to the average value of j_c, then a spontaneous flux and two types of fractional Josephson vortices can be observed. The fractional Josephson vortices keep magnetic fluxes ϕ_1 and ϕ_2, where $\phi_1 + \phi_2 = \phi_0$, ϕ_0 is flux quantum, and $\phi_1 < \phi_0/2$, $\phi_2 > \phi_0/2$. We demonstrate that these fractional vortices can be observed in thin-YBCO films under conditions of appearance of the spontaneous magnetic flux. A method is proposed to extract the fractional vortices from the experimental flux patterns. Propagation of an electromagnetic wave along a grain boundary with an alternating critical current density is treated as an example of an application of the integro-differential equation for the phase difference φ.

1. Introduction

Grain boundaries in thin films of high-temperature superconductors are of great interest and importance for fundamental physics and applications of superconductivity [1–4]. In particular, a notable interest in the Josephson properties of the grain boundaries is motivated by experiments treating symmetry of the order parameter [2–5]. In most cases a model of a strongly coupled SIS-type Josephson junction allows the description of the electromagnetic properties of the grain boundaries in high-temperature superconductors [6, 7]. The tunnel junctions in thin films separate two thin-film banks (grains) from touching each other along the edges. This experimental set-up is quite different from the standard set-up for bulk junctions. Indeed, the stray field outside the film becomes an important factor, this field even governs the phase difference spatial distribution if the film thickness $d < \lambda$, where λ is the London penetration depth [8, 9]. In other words, the Josephson electrodynamics is nonlocal if $d < \lambda$, and instead of a local sine-Gordon equation for a bulk junction an integro-differential equation has to be solved to find the phase difference across a junction in a thin film [8–10].

In some cases an intrinsic inhomogeneity of the Josephson properties of the gain boundaries in the cooper oxide superconductors becomes fundamentally important. In particular, an intrinsic inhomogeneity results in unprecedented Josephson properties discovered for asymmetric 45° [0 0 1]-tilt boundaries in YBCO films [11–15]. First, these junctions demonstrate an anomalous dependence of the critical current I_c on an applied magnetic field H_a. The pattern $I_c(H_a)$ has no standard major central peak at $H_a = 0$, instead, two symmetric major side-peaks appear at certain magnetic fields $H_a = \pm H_{sp} \neq 0$ [11–16]. Second, spontaneous randomly distributed magnetic flux has been discovered at asymmetric 45° [0 0 1]-tilt grain boundaries in YBCO superconducting films in zero-field cooled samples [17]. This flux $\phi_s(y)$ changes its sign randomly (y-axis is along the grain boundary line) and has an amplitude of variations less than

the flux quantum ϕ_0, the average value of $\phi_s(y)$ is nearly zero.

Two fundamental observations result in a model to consider Josephson properties of asymmetric 45° [0 0 1]-tilt grain boundary in YBCO films [14, 15]. First, a fine scale faceting of grain boundaries was found, the facets have a typical length-scale of order of 10–100 nm and a variety of orientations [4, 18–21]. Second, quite a few experiments provide evidence of a predominant $d_{x^2-y^2}$ wave symmetry of the order parameter in many of the high-T_c cuprates; some studies demonstrate that this symmetry is more complicated and is a mixture of $d_{x^2-y^2}$ and s-wave components [2, 3, 22–28].

Next consider a film of a $d_{x^2-y^2}$ wave superconductor with a meandering grain boundary carrying a certain magnetic flux. In this case there is a difference of phases of the order parameter across the boundary caused by the magnetic flux φ and at the same time there is an additional phase difference α caused by the misalignment of the $d_{x^2-y^2}$ wave superconducting grains. The Josephson current density $j(y)$ depends on the total phase difference $\varphi(y) + \alpha(y)$, a model for $j(y)$ results from an assumption that $j(y) \propto \sin[\varphi(y)+\alpha(y)]$ [15]. The phase $\alpha(y)$ depends on the relative orientation of neighbouring facets. The asymmetric 45° [0 0 1]-tilt grain boundaries in YBCO films prescribe $\alpha(y) = 0$ or π and $j(y) = j_c(y)\sin\varphi(y)$ with an *alternating* critical current density $j_c(y) \propto \cos\alpha(y)$ [15].

The basic features of the local Josephson electrodynamics of an asymmetric 45° [0 0 1]-tilt grain boundary in YBCO films with $d > \lambda$ were considered analytically and numerically in the framework of an alternating critical current density model. A criterion of existence of a stationary state with a spontaneous flux was derived assuming that the junction length $L \gg l$ and the local Josephson penetration depth $\lambda_{\rm loc} \gg l$ [29, 30]. It is important to mention that the same alternating dependencies $j_c(y)$ result in anomalous patterns $I_c(H_a)$ [16].

In this paper we consider the nonlinear integro-differential equation for the phase difference $\varphi(y)$ in the case of a Josephson junction in a thin film with a spatially varying critical current density, i.e. for $d \ll \lambda$ and $j_c = j_c(y)$. Special attention is given to the case of a critical current density alternating along the junction. It is shown that if the typical amplitude of alternations of $j_c(y)$ is high compared to the average value of $j_c(y)$, then a spontaneous flux and two types of fractional Josephson vortices can be observed under the same conditions. These fractional vortices keep magnetic fluxes ϕ_1 and ϕ_2, and are complimentary as $\phi_1 + \phi_2 = \phi_0$, where ϕ_0 is flux quantum, and $\phi_1 < \phi_0/2$, $\phi_2 > \phi_0/2$. An electromagnetic wave propagating along a grain boundary is treated using the nonlinear integro-differential equation for $\varphi(y)$.

2. Main equations

In this section we derive briefly the integro-differential equation to study the stationary Josephson properties of grain boundaries in thin film including the case of a critical current density alternating along the grain boundary. Consider a thin film (x, y plane) with a Josephson junction crossing this film along the y-axis. The stray magnetic field significantly influences the spatial distribution of the phase difference $\varphi(y)$ if $d \ll \lambda$. As a result an effective method to derive an equation for $\varphi(y)$ is to solve the spatial distribution of magnetic field $\boldsymbol{h}(\boldsymbol{r})$ and current density $\boldsymbol{j}(\boldsymbol{r})$ inside and outside the film [10]. In the following we use this method for the case of a nonuniform critical current density $j_c(y)$ and, in particular, for an alternating $j_c(y)$.

Outside the film we have $\operatorname{curl}\boldsymbol{h} = \operatorname{div}\boldsymbol{h} = 0$ and, therefore, it is convenient to introduce a scalar potential $\psi(\boldsymbol{r})$ for the *outside* field

$$\boldsymbol{h} = \nabla\psi \qquad \nabla^2\psi = 0. \tag{1}$$

The general form of a solution of equation (1) vanishing at $z \to \pm\infty$ is

$$\psi(\boldsymbol{r}, z) = \int \frac{\mathrm{d}^2\boldsymbol{k}}{(2\pi)^2}\,\psi(\boldsymbol{k})\,\mathrm{e}^{\mathrm{i}\boldsymbol{k}\cdot\boldsymbol{r}-k|z|} \tag{2}$$

where $\boldsymbol{k} = (k_x, k_y)$, $\boldsymbol{r} = (x, y)$, $k = |\boldsymbol{k}|$, and $\psi(\boldsymbol{k})$ is the two-dimensional Fourier transform of $\psi(\boldsymbol{r}, z = 0)$. In order to find a boundary condition for equations (1) and (2) we consider first the current and magnetic field inside the superconductor.

The London equation everywhere in the film except the junction reads as

$$\boldsymbol{h} + \frac{4\pi\lambda^2}{c}\operatorname{curl}\boldsymbol{j} = 0. \tag{3}$$

A similar equation for the two-dimensional sheet current density $\boldsymbol{g} = (g_x, g_y, 0)$ follows from equation (3) after averaging it over the film thickness

$$\boldsymbol{h} + \frac{4\pi\Lambda}{c}\operatorname{curl}\boldsymbol{g} = 0 \tag{4}$$

where $\Lambda = \lambda^2/d$ is the Pearl length [31]. At the junction line $x = 0$, the sheet current component g_y is discontinuous. It is convenient to include this discontinuity into equation (4) and to proceed with an equation which is valid for the whole sample

$$h_z + \frac{4\pi\Lambda}{c}\operatorname{curl}_z\boldsymbol{g} = \frac{\phi_0}{2\pi}f(y)\,\delta(x) \tag{5}$$

where the function $f(y)$ is to be determined. Integration of equation (5) from $x = -0$ to $x = +0$ links $f(y)$ to the sheet current discontinuity

$$f(y) = \frac{8\pi^2\Lambda}{c\phi_0}[g_y(+0, y) - g_y(-0, y)]. \tag{6}$$

Now we use the London relation for the sheet current density

$$\boldsymbol{g} = -\frac{c\phi_0}{8\pi^2\Lambda}\left(\nabla\theta + \frac{2\pi}{\phi_0}\boldsymbol{A}\right) \tag{7}$$

where θ is the phase of the order parameter, $\varphi = \theta(+0, y) - \theta(-0, y)$ is the phase difference across the junction, $\boldsymbol{h} = \operatorname{curl}\boldsymbol{A}$, $\boldsymbol{A}$ is the vector potential, $\boldsymbol{A}(+0, y) = \boldsymbol{A}(-0, y)$. It follows then from equations (6) and (7) that $f(y) = \varphi\prime(y)$.

The final form of equation (5) is obtained by replacing the sheet currents g_x and g_y by the tangential magnetic fields h_x and h_y

$$g_x = -\frac{c}{2\pi}h_y(x, y, +0) \qquad g_y = \frac{c}{2\pi}h_x(x, y, +0) \tag{8}$$

and continuity equation $\operatorname{div} \boldsymbol{h} = 0$. A simple calculation results in

$$h_z - 2\Lambda \frac{\partial h_z}{\partial z} = \frac{\phi_0}{2\pi}\,\delta(x)\,\frac{\mathrm{d}\varphi}{\mathrm{d}y}. \tag{9}$$

The two-dimensional Fourier transform of equation (9) yields

$$\psi(\boldsymbol{k}) = -\frac{\phi_0\,\tilde{\varphi}'(k_y)}{2\pi k(1+2k\Lambda)} \tag{10}$$

where $\tilde{\varphi}'(k_y)$ is the Fourier transform of $\mathrm{d}\varphi/\mathrm{d}y$. The stray field in terms of the phase difference $\varphi(y)$ is given by (10) and thus

$$\psi(\boldsymbol{r}, z) = -\int \frac{\mathrm{d}^2\boldsymbol{k}}{(2\pi)^2}\,\frac{\phi_0\,\tilde{\varphi}'(k_y)\mathrm{e}^{-kz}}{2\pi k(1+2k\Lambda)}\,\mathrm{e}^{\mathrm{i}\boldsymbol{k}\cdot\boldsymbol{r}}. \tag{11}$$

To obtain an equation for $\varphi(y)$, we use the current continuity condition at $x = 0$

$$j_c(y)d\,\sin\varphi(y) = g_x(0, y) = -\frac{c}{2\pi}\,h_y(0, y, +0). \tag{12}$$

It follows from equations (11) and (12) that

$$j_c(y)\sin\varphi(y) = \frac{c\phi_0}{4\pi^2 d}\int \frac{\mathrm{d}^2\boldsymbol{k}}{4\pi^2}\,\frac{\tilde{\varphi}''(k_y)}{k(1+2k\Lambda)}\,\mathrm{e}^{\mathrm{i}k_y y}. \tag{13}$$

We substitute now the inverse Fourier transform for φ'' into equation (13) and obtain an integro-differential equation for $\varphi(y)$ in the final form

$$[1+g(y)]\sin\varphi(y) = \ell_0\int_{-\infty}^{\infty}\mathrm{d}s\,\varphi''(s)\,Q\left(\frac{|y-s|}{2\Lambda}\right) \tag{14}$$

where for convenience we write the critical current density as

$$j_c(y) = \langle j_c\rangle\,[1+g(y)] \tag{15}$$

$\langle j_c\rangle$ is the average value of the critical current density. The dimensionless function $g(x)$ characterizes the variation of $j_c(y)$, the average value $\langle g\rangle = 0$,

$$\ell_0 = \frac{c\phi_0}{16\pi^2\langle j_c\rangle\lambda^2} \tag{16}$$

$$Q(\eta) = \frac{1}{2}\,[\boldsymbol{H}_0(\eta) - Y_0(\eta)] = \frac{1}{\pi}\int_0^{\infty}\mathrm{d}t\,\frac{\mathrm{e}^{-\eta t}}{\sqrt{1+t^2}} \tag{17}$$

$\boldsymbol{H}_0$, Y_0 are Struve and second-kind Bessel functions [32].

Thus, the main integro-differential equation (14) allows us to consider the stationary Josephson properties of grain boundaries in thin films ($d \ll \lambda$) including the case of an alternating critical current density $j_c(y)$.

It follows from equation (14) that the electrodynamics of Josephson junctions in thin films is characterized by two independent lengths ℓ_0 and Λ. In a very thin film, i.e., for $\ell_0 \ll \Lambda$, the main contribution to the integral (14) results from a narrow vicinity of the point $s = y$ and equation (14) can be rewritten as [8]

$$[1+g(v)]\sin\varphi(v) = \frac{1}{\pi}\int_{-\infty}^{\infty}\frac{\mathrm{d}s}{s-v}\,\varphi'(s) \tag{18}$$

where the dimensionless variable $v = y/\ell_0$.

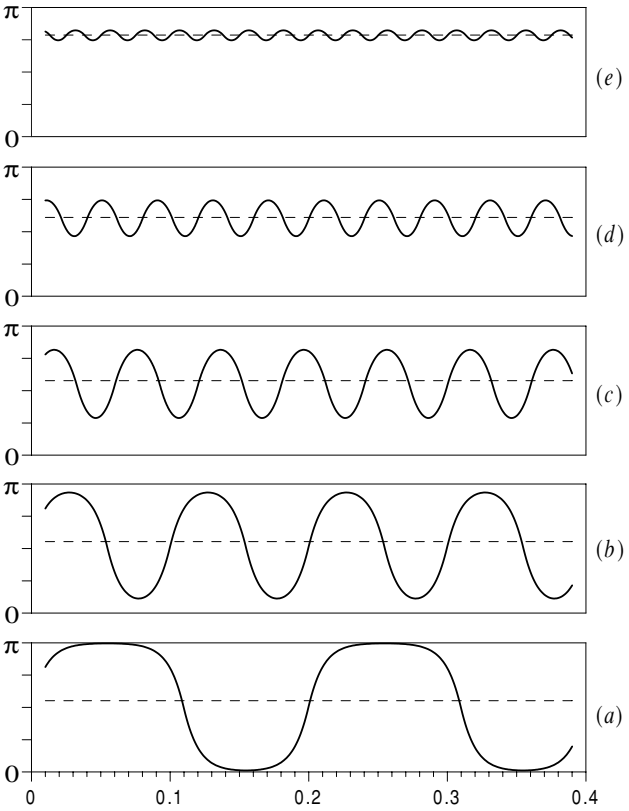

Figure 1. Transformation of the phase difference $\varphi(y)$ from a function generated by a chain of single π-vortices and π-antivortices (curve (*a*)) to a function being a sum of a smooth phase shift ψ (dashed line) and a small rapidly alternating phase $\xi(y)$ (curve (*e*)). The typical length scale of faceting l changes from $l \gg \lambda_{\mathrm{loc}}$ (curve (*a*)) to $l \ll \lambda_{\mathrm{loc}}$ (curve (*e*)). The graphs shown in figures (*a*)–(*e*) have been computed numerically using equation (36) to model a Josephson junction with a fixed length.

3. Spontaneous flux

In this section we consider spontaneous flux patterns in a line Josephson junction in a thin film. We assume that $\lambda \ll l \ll \ell_0, \Lambda$ and treat the case of a periodic alternating critical current density $j_c(y)$ with a period of order of l.

The spatial distribution of the phase $\varphi(y)$ strongly depends on the relation between the length-scale of facetting l and the local Josephson length

$$\lambda_{\mathrm{loc}} = \sqrt{\frac{c\phi_0}{16\pi^2\lambda\,\langle|j_c(y)|\rangle}}. \tag{19}$$

In the case of $l \gg \lambda_{\mathrm{loc}}$ in the stationary state with a minimal Josephson energy almost-single π-vortices are located at the points where the misalignment phase $\alpha(y)$ changes from 0 to π and almost-single π-antivortices are located at the points where $\alpha(y)$ changes from π to 0 [33]. The phase $\varphi(y)$ generated by the chain of the interchanging π-vortices and π-antivortices is shown by a solid line in figure 1(*a*). In the opposite case of $l \ll \lambda_{\mathrm{loc}}$ the phase difference $\varphi(y)$ transforms to a sum of a smooth phase shift ψ (dashed line) and a small rapidly alternating phase $\xi(y)$ as shown in figure 1(*e*). As a result this case allows for the two-scale perturbation theory approach [34].

3.1. Two-scale perturbation theory approach

We follow now the two-scale perturbation theory approach [34] and write $\varphi(y)$ as a sum of a smooth function $\psi(y)$ with a length scale much bigger than l and a small but rapidly oscillating function $\xi(y)$ with a length scale of the order of l, i.e.,

$$\varphi(y) = \psi(y) + \xi(y) \tag{20}$$

where $|\xi(y)| \ll |\psi(y)|$. Next we substitute equation (20) into equation (14), keep the terms up to the first order in $|\xi(y)| \ll 1$, and arrive at the following equation:

$$\left[\sin\psi + \xi g\cos\psi - \ell_0\int_{-\infty}^{\infty} \mathrm{d}s\,\psi''(s)\,Q\left(\left|\frac{y-s}{2\Lambda}\right|\right)\right] + \left[g\sin\psi - \ell_0\int_{-\infty}^{\infty}\mathrm{d}s\,\xi''(s)\,Q\left(\left|\frac{y-s}{2\Lambda}\right|\right)\right] = 0. \tag{21}$$

The terms included in the first pair of brackets in equation (21) cancel each other independently on the terms included into the second pair of brackets in equation (21) as the two types of terms have very different typical length scales [34]. The same reasoning is applicable to the terms included in the second pair of brackets in equation (21). As a result we arrive at a pair of integro-differential equations for $\psi(y)$ and $\xi(y)$

$$\ell_0\int_{-\infty}^{\infty}\mathrm{d}s\,\psi''(s)\,Q\left(\left|\frac{y-s}{2\Lambda}\right|\right) = \sin\psi + \langle\xi(y)g(y)\rangle\cos\psi \tag{22}$$

$$\ell_0\int_{-\infty}^{\infty}\mathrm{d}s\,\xi''(s)\,Q\left(\left|\frac{y-s}{2\Lambda}\right|\right) = g(y)\sin\psi. \tag{23}$$

It is important that in spite of the fact that both functions $g(y)$ and $\xi(y)$ are rapidly oscillating the product $\xi(y)g(y)$ has both smooth and rapid contributions. The smooth part of $\xi(y)g(y)$ is given by the average $\langle\xi(y)g(y)\rangle$ which eliminates the rapid alternations. The second term in the right-hand side of equation (22) represents the contribution of the smooth part of the product $\xi(y)g(y)$. We obtain *two* equations for the *two* functions $\psi(y)$ and $\xi(y)$ from *one* equation (21) as only two types of terms with very different typical length scales appear in equation (21). If $g(y)$ had a wide range of typical length scales the above separation would not be possible.

In the case of $\ell_0 \gg \Lambda$ (a relatively thick film with $\lambda \ll \Lambda \ll \ell_0$) the complexity of the system of integro-differential equations (22) and (23) can significantly be reduced. Indeed, we write

$$\xi(y) = -\xi_g(y)\sin\psi \tag{24}$$

plug this relation into equation (23), and obtain an equation for the function $\xi_g(y)$

$$\ell_0\int_{-\infty}^{\infty}\mathrm{d}s\,\xi_g''(s)\,Q\left(\left|\frac{y-s}{2\Lambda}\right|\right) + g(y) = 0. \tag{25}$$

Using relation (24) we transform equation (22) for the function $\psi(y)$ to its final form

$$\ell_0\int_{-\infty}^{\infty}\mathrm{d}s\,\psi''(s)\,Q\left(\left|\frac{y-s}{2\Lambda}\right|\right) - \sin\psi(1-\gamma\cos\psi) = 0 \tag{26}$$

where the dimensionless constant $\gamma > 0$ is given by

$$\gamma = \langle g(y)\xi_g(y)\rangle = \ell_0\left\langle\int_{-\infty}^{\infty}\mathrm{d}s\,\xi_g'(y)\xi_g'(s)\,Q\left(\left|\frac{y-s}{2\Lambda}\right|\right)\right\rangle \tag{27}$$

In the opposite case of $\ell_0 \ll \Lambda$, i.e., for a very thin film we obtain two equations for $\psi(y)$ and $\xi(y)$ by means of equation (18). Indeed, we substitute equation (20) into equation (18), keep the main terms in $|\xi(y)| \ll 1$, and we arrive at

$$\frac{1}{\pi}\int_{-\infty}^{\infty}\frac{\mathrm{d}s}{s-v}\,\psi'(s) = \sin\psi + \langle\xi(y)g(y)\rangle\cos\psi \tag{28}$$

and

$$\frac{1}{\pi}\int_{-\infty}^{\infty}\frac{\mathrm{d}s}{s-v}\,\xi'(s) = g\sin\psi \tag{29}$$

where we introduced a dimensionless variable $v = y/\ell_0$.

3.2. Spontaneous flux

To fix ideas we now assume that $\ell_0 \ll \Lambda$ and consider a simple model dependence

$$g(y) = g_0\sin\left(\frac{2\pi y}{l}\right). \tag{30}$$

In this case $\xi_g(y) \propto g(y)$ and we have

$$\xi_g(y) = \xi_0\sin\left(\frac{2\pi y}{l}\right) \tag{31}$$

where the amplitude ξ_0 is determined by equation (25). A simple integration results in

$$\xi_0 = \frac{g_0}{4\pi}\,\frac{l}{\ell_0} \qquad \gamma = \frac{g_0^2}{8\pi}\,\frac{l}{\ell_0}. \tag{32}$$

Next, we treat the stationary states of a Josephson junction in the absence of an applied magnetic field. In this case the total flux inside the junction is zero, the alternating spontaneous flux $\phi_s(y) = \phi_0\xi(y)/2\pi$ appears simultaneously with a certain phase difference $\psi = \text{const}$, and the value of ψ is determined by equation (26) which yields

$$\sin\psi\,(1-\gamma\cos\psi) = 0. \tag{33}$$

Note that this equation also means that the average value of the tunnel current density $j(y)$ across the junction is equal to zero.

In the case of $\gamma < 1$ equation (33) has two solutions: $\psi = 0,\ \pi$. It follows then from equation (24) that there is no spontaneous flux. It is worth noting that the energy of a Josephson junction $\mathcal{E}$ [35] has a minimum for $\psi = 0$ and a maximum for $\psi = \pi$. In the case of $\gamma \geqslant 1$ equation (33) has four solutions: $\psi = -\psi_\gamma,\ 0,\ \psi_\gamma,\ \pi$, where

$$\psi_\gamma = \arccos(1/\gamma). \tag{34}$$

The Josephson energy $\mathcal{E}$ has a minimum for $\psi = \pm\psi_\gamma$ and a maximum for $\psi = 0, \pi$ [29], and the spontaneous flux

$$\phi_s = \frac{\phi_0\xi}{2\pi} = -\frac{\phi_0\xi_g}{2\pi}\sin\psi_\gamma = \mp\phi_0\frac{g_0}{8\pi^2}\,\frac{l}{\ell_0}\,\frac{\sqrt{\gamma^2-1}}{\gamma}\,\sin\left(\frac{2\pi y}{l}\right) \tag{35}$$

arises in the two stationary states with $\psi = \pm\psi_\gamma$.

The above analytical approach to the problem of spontaneous flux in a Josephson junction is based on the assumption that the critical current density $j_c(y)$ is an alternating periodic function. This simple model provides a reasonable preliminary insight into the properties of an idealized Josephson junction with an alternating $j_c(y)$. However, this approach fails as a quantitative description of any real system having a certain randomness of the spatial distribution of the critical current density $j_c(y)$.

To illustrate the qualitative difference between the spontaneous flux in the cases of a periodic and random functions $j_c(y)$ we refer to a numerical calculation valid for a thick film ($d \gg \lambda$). The problem then can be solved by means of a time-dependent sine-Gordon equation [30]

$$\ddot{\varphi} + \alpha\dot{\varphi} - \varphi'' + [1 + g(y)]\sin\varphi = 0 \qquad (36)$$

where α is a decay constant. The term $\alpha\dot{\varphi}$ introduces dissipation which results in a relaxation of the system towards one of the stable stationary states, i.e., this approach allows us to study both the dynamics and the statics of the system. To solve equation (36) numerically we took $\alpha \sim 1$ and use the finite difference scheme [36]. We adopted this method in our case and checked stability and convergency of the obtained solutions.

In particular, now consider the flux patterns for a case of a grain boundary with *2N* facets and a non-periodic alternating critical current density $j_c(y)$. We treat this case numerically using a stepwise function $g(y)$ defined as: $g(y) = g_0$ if $a_i < y < b_i$, and $g(y) = -g_0$ if $b_i < y < a_{i+1}$ ($i = 1, \ldots, N$). It is convenient to introduce the random distances $\tilde{a}_i$ and $\tilde{b}_i$ with $\langle\tilde{a}_i\rangle = \langle\tilde{b}_i\rangle = 0$ and a standard deviation σ_l such that $b_i - a_i = 0.5(l + \tilde{a}_i)$ and $a_{i+1} - b_i = 0.5(l + \tilde{b}_i)$. The simulations start with an initial phase $\varphi_i(y)$ matching the condition of a given total flux.

The stationary state $\varphi_s(y)$ corresponding to the zero total spontaneous flux has a special role in the description of Josephson boundaries with random alternating $j_c(y)$. Our simulations show that in this case the function $\varphi_s(y)$ is *unique* for a given boundary, *stable*, and *independent* of the initial guess $\varphi_i(y)$. It is convenient to represent $\varphi_s(y)$ as $\varphi_s(y) = \psi_\gamma + \xi_s(y)$ with $\psi_\gamma = \text{const}$ and the variable part $\xi_s(y)$ having zero average, $\langle\xi_s(y)\rangle = 0$, and a typical amplitude $|\xi_s(y)| < \pi/2$.

An example of a computed $\varphi_s(y)$ is shown in figure 2. For this simulation we took $\varphi_i(y) = \text{const} + \xi_i(y)$ with an arbitrary small $\xi_i(y)$. As stated above, the resulting phase $\varphi_s(y)$ is independent of $\varphi_i(y)$. It is worth mentioning that the spontaneous self-generated flux $\phi_s(y) = \phi_0\xi_s(y)/2\pi$ has a wide range of length scales imposed by the random $j_c(y)$. The randomness of $j_c(y)$ results in a considerably higher amplitude of the flux variation $\phi_s(y)$ as compared to a periodic $j_c(y)$ (see equation (35)).

4. Fractional Josephson vortices

In this section we consider Josephson vortices at a grain boundary with a critical current density alternating along the grain boundary. In the framework of the two-scale perturbation theory, a single Josephson vortex is described

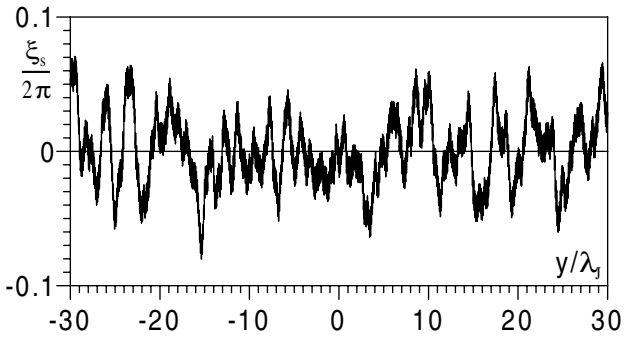

Figure 2. A stationary solution $\xi_s(y)$ developed in a zero applied magnetic field for a stepwise randomly alternating $j_c(y)$ with $g_0 = 200, l = 0.1\,\lambda_J, \sigma_l \approx 0.06l$.

by the smooth phase $\psi(y)$ being a solution of equation (26) under the boundary conditions $\psi'(\pm\infty) = 0$. These boundary conditions transform to $\sin\psi_\pm(1 - \gamma\cos\psi_\pm) = 0$, with $\psi_\pm = \psi(\pm\infty)$, and it is convenient for further analysis to assume that $\psi_- < \psi_+$.

In the case of $\gamma < 1$, equation (26) has one vortex-type solution with a phase $\psi(y)$ increasing monotonically from $\psi_- = 0$ to $\psi_+ = 2\pi$. This solution describes a standard single Josephson vortex with one flux quantum ϕ_0. In the case of $\gamma > 1$, equation (26) has two vortex-type solutions, each of them describes a single fractional Josephson vortex. Indeed, for the *first* fractional vortex the phase difference $\psi(y)$ changes from $\psi_- = -\psi_\gamma$ to $\psi_+ = \psi_\gamma$, where ψ_γ is given by equation (34). The total increase of the phase ψ is given by $\psi_+ - \psi_- = 2\psi_\gamma$, i.e., this Josephson vortex carries a fractional flux $\phi_1 = \psi_\gamma\phi_0/\pi < \phi_0/2$. For the *second* fractional vortex $\psi_+ = 2\pi - \psi_\gamma$ and $\psi_- = \psi_\gamma$. The total increase of the phase ψ is given by $2\pi - 2\psi_\gamma$, i.e., this Josephson vortex carries a fractional flux $\phi_2 = (1 - \psi_\gamma/\pi)\phi_0 > \phi_0/2$. These two fractional vortices are *complementary* meaning that $\phi_1 + \phi_2 = \phi_0$.

In our numerical study of fractional Josephson vortices we treat the stationary states and the relaxation to the stationary states using the sine-Gordon equation (36). We begin with an 'ideal' grain boundary with a periodically alternating critical current density $j_c(y)$. The simulations started from a certain initial phase $\varphi_i(y)$ under the condition $\varphi_i(\mathcal{L}) - \varphi_i(0) = 2\pi n$, where n is an integer, the junction length $\mathcal{L} \gg \lambda_J$, and λ_J is the effective Josephson penetration depth given by

$$\lambda_J = \sqrt{\frac{c\phi_0}{16\pi^2\langle j_c\rangle\lambda}}. \qquad (37)$$

In this case the numerical procedure converges well to a final stationary state.

In figure 3 we show a stable stationary solution for a pair of fractional vortices. We compute the function $\varphi(y)$ using the model dependence $g(y) = g_0\sin(2\pi y/l)$ with $g_0 = 100$ and $l = 0.1\lambda_J$, which yields $\gamma \approx 1.27$ and $\psi_\gamma \approx 0.66$; thus $\phi_1 \approx 0.21\,\phi_0, \phi_2 \approx 0.79\,\phi_0$, the numerical simulation gives the same value of ψ_γ. The magnified insets in figure 3 demonstrate that $\varphi(y)$ indeed consists of a smooth part superimposed by a small fast oscillating term, i.e., the numerical simulations for the single fractional vortices confirm the results of the approximate analytic approach described above.

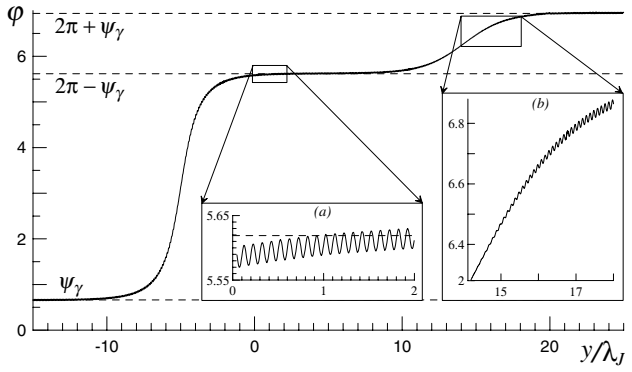

Figure 3. The phase distribution $\varphi(y)$ computed using $g(y) = g_0 \sin(2\pi y/l)$ and $\gamma \approx 1.27$. Two fractional vortices with $\phi_1 \approx 0.21\,\phi_0$ and $\phi_2 \approx 0.79\,\phi_0$ are clearly seen, the fine structure of $\varphi(y)$ is demonstrated in the magnified insets.

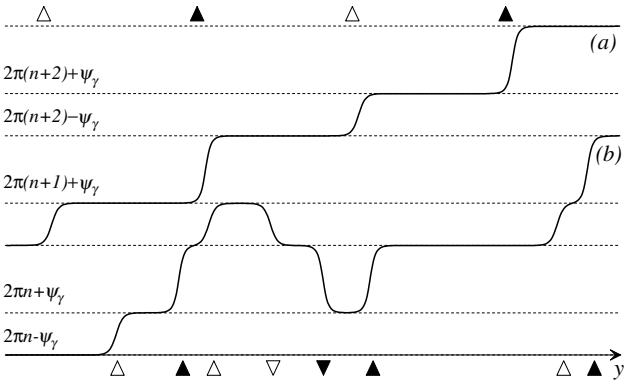

Figure 4. Two chains of fractional vortices in a grain boundary with a periodically alternating critical current density: (*a*) an 'ideal' chain; (*b*) a chain with vortex–antivortex 'defects'. Empty triangles mark the positions of the fractional vortices with the fluxes $\phi_1 < \phi_0/2$, full triangles correspond to $\phi_2 > \phi_0/2$. The up-down orientations of triangles indicate the field direction of vortices. For this particular calculation we use $g(x) = g_0 \sin(2\pi x/l)$, $g_0 = 150$, $l = 0.1\,\Lambda_J$, which result in $\gamma \approx 2.85$, $\psi_\gamma \approx 1.21$, and $\phi_1 \approx 0.39\phi_0$, $\phi_2 \approx 0.61\phi_0$.

Consider now a dilute chain of fractional vortices. Let a vortex with the flux ϕ_1 be situated somewhere in the chain. The phase ψ of this vortex changes from $2\pi n - \psi_\gamma$ to $2\pi n + \psi_\gamma$ with an integer n. Therefore, one expects the phase of an adjacent vortex to start with the value $2\pi n + \psi_\gamma$ and end up with $2\pi(n+1) - \psi_\gamma$, the total phase accumulation of these two vortices being 2π. In other words, the chain consists of a sequence of pairs of vortices with fluxes ϕ_1 and ϕ_2. This qualitative picture is confirmed by numerically solving equation (36). Figure 4(*a*) shows the result of such a calculation for which we took $g(x) = 150\,\sin(20\,\pi x/\Lambda_J)$, that corresponds to $\gamma \approx 2.85$, $\psi_\gamma \approx 1.21$, and the fluxes $\phi_1 \approx 0.39\phi_0$, $\phi_2 \approx 0.61\phi_0$. The final stationary state of our numerical procedure simulating the relaxation process depends on the choice of the initial phase $\varphi_i(x)$. By taking a proper non-monotonic dependence $\varphi_i(x)$, we may end up with a stationary solution shown in figure 4(*b*). A remarkable feature of this solution is the existence of *fractional vortex–antivortex pairs* clearly seen in the simulation of figure 4(*b*), the pair with the fluxes $\pm\phi_1$ is followed by the pair with $\mp\phi_2$.

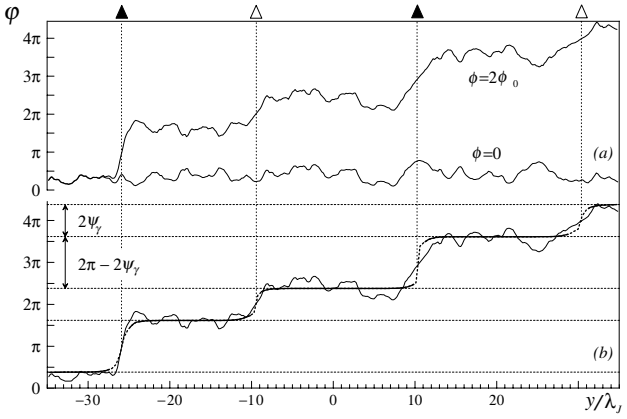

Figure 5. (*a*) The phases $\varphi_s(y)$ with the total flux $\phi = 0$ and $\varphi(y)$ with the total flux $\phi = 2\phi_0$ calculated for $g_0 = 90$, $l = 0.1\,\lambda_J$, $\sigma_l \approx 0.015l$, which gives $\psi_\gamma \approx 1.21$, and $\phi_1 \approx 0.39\phi_0$, $\phi_2 \approx 0.61\phi_0$. (*b*) The thin line depicts $\varphi(y)$, the thick line depicts the phase $\varphi_v(y)$ generated by the fractional vortices and extracted from the phase $\varphi(y)$.

Next we consider a flux pattern for a chain of vortices in the case of a randomly alternating critical current density $j_c(y)$. Assume that this chain starts with a region where the phase is given by $\varphi_s(y) = \psi_\gamma + \xi_s(y)$, therefore, ψ_γ is the value of $\langle\varphi(y)\rangle$ at the 'tail' of the neighbouring vortex or antivortex. If the neighbour carries the flux ϕ_2, the average phase should increase from ψ_γ to $2\pi - \psi_\gamma$ in the neighbour's domain. Another option appears if the neighbour carries the flux $-\phi_1$ generating a decrease of the average phase difference $\langle\varphi(y)\rangle$ from ψ_γ to $-\psi_\gamma$.

In figure 5(*a*) we show the curves $\varphi_s(y)$ with a zero total flux and $\varphi(y)$ with a total flux of two flux quanta. The following method allows for subtracting of the fractional Josephson vortices from a 'noise' flux pattern. First, we draw the straight lines $2\pi n \pm \psi_\gamma$ at the graph of $\varphi(y)$ (see figure 5(*b*)). We see that 'random' variations of $\varphi(y)$ are nested on one of these lines everywhere, except a few relatively sharp phase 'jumps' from one line to the next. The Josephson vortices should be centred at $\varphi(y) = \pi n$ where $\varphi''(y) = 0$. Then we take a domain situated between lines πn and $\pi(n+1)$ and form $\varphi_v(y) = \varphi(y) \mp \xi_s(y)$, choosing the minus if the random parts of $\varphi(y)$ and $\varphi_s(y)$ are identical, and the plus otherwise. The curve $\varphi_v(y)$ shown by a thick line at figure 5(*b*) is *smooth* and clearly represents the fractional Josephson vortices.

5. Electromagnetic wave propagating along a grain boundary

In this section we consider an electromagnetic wave propagating along a line Josephson junction with a spatially alternating critical current density. In this case the phase difference φ depends on the coordinate y and time t, and instead of equation (20) we write

$$\varphi(y,t) = \psi(y,t) + \xi(y,t). \tag{38}$$

A straightforward generalization of equations (22) and (23) results in equations for the time-dependent smooth

$\psi(y,t)$ and rapidly alternating $\xi(y,t)$ functions. We assume that $\lambda \ll l \ll l_0$, Λ, and $|\psi(y,t)| \ll |\xi(y,t)|$, take into account the displacement current, and arrive at the system

$$\ell_0 \int_{-\infty}^{\infty} \mathrm{d}s\, \psi''(s,t)\, Q\Big(\Big|\frac{y-s}{2\Lambda}\Big|\Big) = \omega_J^{-2}\ddot{\psi} + \sin\psi + \langle \xi(y) g(y)\rangle \cos\psi \tag{39}$$

$$\ell_0 \int_{-\infty}^{\infty} \mathrm{d}s\, \xi''(s,t)\, Q\Big(\Big|\frac{y-s}{2\Lambda}\Big|\Big) = g(y)\sin\psi \tag{40}$$

where the Josephson frequency ω_J is given by

$$\omega_J^2 = \frac{2e\langle j_c\rangle}{\hbar C} \tag{41}$$

and C is the specific capacitance of the grain boundary.

Consider now an electromagnetic wave propagating along a Josephson junction in the absence of an applied magnetic field. In this case the average flux inside the junction is zero and it is convenient to write solutions of equations (39) and (40) in the form $\xi = -\xi_g(y)\sin\psi_{\mathrm{st}}$, $\psi(y,t) = \psi_{\mathrm{st}} + \zeta(y,t)$, where ψ_{st} is a solution of the stationary equation (22), and $|\zeta(y,t)| \ll 1$. Linearization of equation (39) leads to

$$\ell_0 \int_{-\infty}^{\infty} \mathrm{d}s\, \zeta''(s,t)\, Q\Big(\Big|\frac{y-s}{2\Lambda}\Big|\Big) = \omega_J^{-2}\ddot{\zeta} + \omega_\gamma^2 \zeta \tag{42}$$

the dimensionless parameter ω_γ is given by

$$\omega_\gamma = \begin{cases} \sqrt{1-\gamma} & \text{if} \quad \gamma < 1 \\ \sqrt{\gamma - 1/\gamma} & \text{if} \quad \gamma > 1. \end{cases} \tag{43}$$

In the case of a plane wave we have $\zeta(x,t) \propto \exp(-\mathrm{i}\omega t + \mathrm{i}ky)$. Substituting this relation into equation (42) we obtain a dispersion relation $\omega(k)$ for an electromagnetic wave propagating along a Josephson junction with an alternating critical current density,

$$\omega = \omega_J \sqrt{\omega_\gamma^2 + 2l_0\Lambda k^2 \tilde{Q}(2k\Lambda)} \tag{44}$$

where

$$\tilde{Q}(\eta) = \begin{cases} \frac{1}{\pi\sqrt{1-\eta^2}} \ln\frac{1+\sqrt{1-\eta^2}}{1-\sqrt{1-\eta^2}} & \text{if} \quad \eta < 1 \\ \frac{1}{\sqrt{\eta^2-1}}\left[1 - \frac{2}{\pi}\arctan\frac{1}{\sqrt{\eta^2-1}}\right] & \text{if} \quad 1 \leqslant \eta. \end{cases} \tag{45}$$

It follows from (45) that

$$\tilde{Q}(\eta) \approx \begin{cases} \frac{2}{\pi}\ln\frac{2}{\eta} & \text{if} \quad \eta \ll 1 \\ \frac{1}{\eta} & \text{if} \quad \eta \gg 1 \end{cases} \tag{46}$$

and therefore

$$\omega \approx \omega_j \begin{cases} \sqrt{\omega_\gamma^2 + \frac{4\ell_0\Lambda k^2}{\pi}\ln\frac{1}{k\Lambda}} & \text{if} \quad k\Lambda \ll 1 \\ \omega_J\sqrt{\omega_\gamma^2 + k\ell_0}, & \text{if} \quad k\Lambda \gg 1. \end{cases} \tag{47}$$

The effect of an alternating critical current density on the dispersion relation $\omega(k)$ of an electromagnetic wave propagating along a Josephson junction is most important in a narrow vicinity of $k = 0$, where $\omega \approx \omega_J\omega_\gamma$. The dimensionless parameter ω_γ varies from $\omega_\gamma = 0$ to $\omega_\gamma > 1$ depending on the value of γ. It is worth noting that for $k\Lambda \gg 1$ and $k\ell_0 \gg 1$ we have $\omega(k) \propto \sqrt{k}$. This is a consequence of a small thickness of the film ($d \ll \lambda$) or in other words of the stray field outside the sample [9].

6. Summary

To summarize, we derive an integro-differential equation for the phase difference across a Josephson junction in a thin film in the case of a critical current density rapidly alternating along this junction. A dispersion relation for an electromagnetic wave propagating along a grain boundary is obtained as an example of an application of this integro-differential equation.

We demonstrate that if a typical amplitude of alternations of the critical current density is high compared to its average value, then a spontaneous flux and two types of complementary fractional Josephson vortices can be observed under the same experimental set-up. An effective method is proposed to extract the fractional Josephson vortices from an experimental flux pattern.

References

[1] Chaudhari P and Lin S Y 1994 *Phys. Rev. Lett.* **72** 1084
[2] Tsuei C C and Kirtley J R 2000 *Rev. Mod. Phys.* **72** 969
[3] Tsuei C C, Kirtley J R, Chi C C, Yu-Jhanes Lock See, Gupta A, Shaw T, Sun J Z and Ketchen M B 1994 *Phys. Rev. Lett.* **73** 593
[4] Miller J H, Ying Q Y, Zou Z G, Fan N Q, Xu J H, Davis M F and Wolfe J C 1995 *Phys. Rev. Lett.* **74** 2347
[5] Kirtley J R, Tsuei C C, Rupp M, Sun J Z, Yu-Jahnes Lock See, Gupta A, Ketchen M B, Moler K A and Bhushan M 1996 *Phys. Rev. Lett.* **76** 1336
[6] Chaudhari P, Dimos D and Mannhart J 1989 *IBM J. Res. Dev.* **33** 299
[7] Gross R, Chaudhari P, Dimos D, Gupta A and Koren G 1990 *Phys. Rev. Lett.* **64** 228
[8] Mints R G and Snapiro I B 1994 *Phys. Rev.* B **49** 6188
[9] Mints R G and Snapiro I B 1995 *Phys. Rev.* B **51** 3054
[10] Kogan V G, Dobrovitski V V, Clem J R, Mawatari Yasunori and Mints R G 2001 *Phys. Rev.* B **63** 144501
[11] Ivanov Z G, Alarco J A, Claeson T, Nilsson P-Å, Olsson E, Olsson H K, Stepantsov E A, Tzalenchuk A Ya and Winkler D 1992 *BHTSC'92: Proc. Beijing Int. Conf. on High-Temperature Superconductivity* ed Z Z Gan, S S Xie and Z X Zhao (Singapore: World Scientific) p 722
[12] Chew N G, Goodyear S W, Humphreys R G, Satchell J S, Edwards J A and Keene M N 1992 *Appl. Phys. Lett.* **60** 1516
[13] Humphreys R G, Satchell J S, Goodyear S W, Chew N G, Keene M N, Edwards J A, Barret C P, Exon N J and Lander K 1995 *Proc. 2nd Workshop on HTS Applications and New Materials* ed D H A Blank (Enschede: University of Twente) p 16
[14] Copetti C A, Rüders F, Oelze B, Buchal Ch, Kabius B and Seo J W 1995 *Physica* C **253** 63
[15] Hilgenkamp H, Mannhart J and Mayer B 1996 *Phys. Rev.* B **53** 14586
[16] Mints R G and Kogan V G 1999 *Phys. Rev.* B **55** 8682
[17] Mannhart J, Hilgenkamp H, Mayer B, Gerber Ch, Kirtley J R, Moler K A and Sigrist M 1996 *Phys. Rev. Lett.* **77** 2782
[18] Jia C L, Kabius B, Urban K, Herrmann K, Schubert J, Zander W and Braginski A I 1992 *Physica* C **196** 211
[19] Rosner S J, Char K and Zaharchuk G 1992 *Appl. Phys. Lett.* **60** 1010
[20] Traeholt C, Wen J G, Zandbergen H W, Shen Y and Hilgenkamp J W M 1994 *Physica* C **230** 425
[21] Seo J W, Kabius B, Dähne U, Scholen A and Urban K 1995 *Physica* C **245** 25
[22] Miller D J, Roberts T A, Kang J H, Talvacchio J, Buchholz D B and Chang R P H 1995 *Appl. Phys. Lett.* **66** 2561
[23] Wollman D A, Van Harlingen D J, Lee D J, Lee W C, Ginsberg D M and Legget A J 1993 *Phys. Rev. Lett.* **71** 2134

[24] Brawner D A and Ott H R 1994 *Phys. Rev.* B **50** 6530
[25] Iguchi I and Wen Z 1994 *Phys. Rev.* B **49** 12 388
[26] Van Harlingen D J 1995 *Rev. Mod. Phys.* **67** 515
[27] Ishimaru Y, Wen J, Hayashi K, Enomoto Y and Koshizuka N 1995 *Japan. J. Appl. Phys.* **34** L1532
[28] Müller K A 1995 *Nature* **377** 133
[29] Mints R G 1998 *Phys. Rev.* B **57** 3221
[30] Mints R G and Papiashvili I 2000 *Phys. Rev.* B **62** 15214
[31] Pearl J 1964 *Appl. Phys. Lett.* **5** 65
[32] Gradshteyn I S and Ryzhik I M 1980 *Tables of Integrals, Series and Products* (New York: Academic)
[33] Xu J H, Miller J H and Ting C S 1995 *Phys. Rev. Lett.* **51** 11958
[34] Landau L D and Lifshitz E M 1994 *Mechanics* (Oxford: Pergamon) p 93
[35] Barone A and Paterno G 1982 *Physics and Applications of the Josephson Effect* (New York: Wiley)
[36] Ablowitz M J, Kruskal M D and Ladic J F 1997 *SIAM J. Appl. Math.* **36** 428